Developmental Biology 395 (2014) 287–298

Contents lists available at ScienceDirect

Developmental Biology

journal homepage: www.elsevier.com/locate/developmentalbiology

Chibby functions in *Xenopus* ciliary assembly, embryonic development, and the regulation of gene expression

Jianli Shi, Ying Zhao, Domenico Galati [1], Mark Winey, Michael W. Klymkowsky *

Molecular, Cellular, & Developmental Biology, University of Colorado, Boulder, CO 80309-347, USA

ARTICLE INFO

Article history:
Received 30 April 2014
Received in revised form
3 September 2014
Accepted 5 September 2014
Available online 16 September 2014

Keywords:
Chibby
Cilia
Snail2
Wnt signaling
Hedgehog
Xenopus laevis
Neural crest
Neural plate
Pronephros

ABSTRACT

Wnt signaling and ciliogenesis are core features of embryonic development in a range of metazoans. Chibby (Cby), a basal-body associated protein, regulates β-catenin-mediated Wnt signaling in the mouse but not *Drosophila*. Here we present an analysis of Cby's embryonic expression and morphant phenotypes in *Xenopus laevis*. *Cby* RNA is supplied maternally, negatively regulated by Snail2 but not Twist1, preferentially expressed in the neuroectoderm, and regulates β-catenin-mediated gene expression. Reducing Cby levels reduced the density of multiciliated cells, the number of basal bodies per multiciliated cell, and the numbers of neural tube primary cilia; it also led to abnormal development of the neural crest, central nervous system, and pronephros, all defects that were rescued by a Cby-GFP chimera. Reduction of Cby led to an increase in *Wnt8a* and decreases in *Gli2*, *Gli3*, and *Shh* RNA levels. Many, but not all, morphant phenotypes were significantly reversed by the Wnt inhibitor SFRP2. These observations extend our understanding of Cby's role in mediating the network of interactions between ciliogenesis, signaling systems and tissue patterning.

Introduction

Different organisms develop in mechanistically different ways and homologous proteins can have distinctly different physiological roles in different contexts. These differences presumably reflect the range of functional roles a specific protein can play. Chibby (Cby) provides an interesting example of this principle. Cby is a small (108–125 amino acids), evolutionarily conserved protein associated with basal bodies and involved in ciliogenesis (see (Enjolras et al., 2012)). Based on Blast searches, Cby is apparently absent from unicellular eukaryotes and sponges (data not shown). Cby has been localized to the distal end of mother centrioles in a range of cultured vertebrate cell lines and found to interact with Cenexin1, a splice variant of the outer dense fiber 2 (*Odf2*) gene, a protein involved in primary cilia formation (Ishikawa et al., 2005; Steere et al., 2012; Chang et al., 2013). Cenexin1 in turn interacts with Rab8a GTPase (Yoshimura et al., 2007) and is involved in the coordinated beating of epithelial cilia (Kunimoto et al., 2012). In mammalian cells and *Xenopus laevis* embryos (this work), but not in *Drosophila* (Enjolras et al., 2012), Cby acts as a negative regulator of canonical, that is, β-catenin-mediated Wnt signaling (Takemaru et al., 2003, 2009). Cby appears to form a homodimer in solution; structural studies indicate that its N-terminal domain is unstructured while its C-terminal region forms an α-helical coiled-coil (Mofunanya et al., 2009; Mokhtarzada et al., 2011). A C-terminal extension present in hydra, *Xenopus*, mouse, and human, but not *Drosophila* Cby proteins (supplemental Fig. S1) could be involved in this signaling role. Cby's interaction with β-catenin appears to involve a complex with 14-3-3 proteins and leads to β-catenin's export from the nucleus, inhibiting its interactions with LEF1/TCF-type HMG-box transcription factors (Li et al., 2010). The Cby-driven cytoplasmic accumulation of β-catenin has been reported to induce an unfolded protein response (Mancini et al., 2013). TC1 (C8orf4), a protein originally identified based on its over-expression in thyroid cancer cells (Chua et al., 2000; Sunde et al., 2004), interacts with and inhibits Cby's interactions with β-catenin, thereby enhancing canonical Wnt signaling (Jung et al., 2006). The dynamics of the Cby-C8orf4 (TC1) interaction and its physiological significance have yet to be characterized. Finally, other binding partners of Cby have been identified (Vandepoele et al., 2010), but again their physiological significance has yet to be resolved. In addition to Cby, β-catenin also interacts with a subset

Abbreviations: RT-PCR, reverse transcription, polymerase chain reaction; MO, morpholino; AAT, acetylated α-tubulin; qPCR, quantitative reverse transcription, polymerase chain reaction.

* Corresponding author.
E-mail address: michael.klymkowsky@colorado.edu (M.W. Klymkowsky).
[1] Current address: Cell and Developmental Biology, University of Colorado, Denver 12801 E. 17th Avenue, Aurora, CO 80045, USA.

http://dx.doi.org/10.1016/j.ydbio.2014.09.008
0012-1606/

of Sox-type HMG-box transcription factors (Zorn et al., 1999; Zhang et al., 2003). These proteins play a role in the regulation of embryonic patterning (Kanai-Azuma et al., 2002; Avilion et al., 2003; Zhang and Klymkowsky 2007), have been used to reprogram somatic cells to form induced pluripotent stem cells (Takahashi et al., 2007), and have complex regulatory effects on canonical Wnt signaling (Sinner et al., 2004; Kormish et al., 2010), raising the possibility that Cby regulation of β-catenin could influence a range of molecular systems beyond Wnt signaling.

cby$^{-/-}$ mice (in a C57BL/6 background) develop in a grossly normal manner (Voronina et al., 2009), a surprising result for a protein involved in both ciliogenesis and the regulation of Wnt signaling. That said, approximately 75% of *cby*$^{-/-}$ animals died within two weeks of birth and were "runted and demonstrated anemia." The remaining ~25% subsequently gained weight and survived for more than 18 months (Voronina et al., 2009). Analysis of *cby*$^{-/-}$ mice indicated that they were susceptible to sinus and middle ear infections and that their mucociliary transport rate was essentially zero. *cby*$^{-/-}$ mice also displayed a number of structural defects in their lungs, specifically a reduction in the percentage of multi-ciliated epithelial cells, an increase in the percentage of secretory (Clara) cells, and an increase in β-catenin-dependent gene expression activity (Love et al., 2010). Over-expression of Cby has been found to drive cardiomyocyte differentiation in murine embryonic stem cells (Singh et al., 2007), although heart abnormalities were not reported in *cby*$^{-/-}$ mice.

Cby's roles in non-mammalian vertebrates have not yet been established. The *Xenopus laevis* embryo offers an alternative developmental system within which to characterize the biological roles of Cby. The experimental analysis of *X. laevis* development can reveal molecular behaviors and cellular roles obscure in other contexts (see Sive, 2011). Ectodermal explants differentiate into ciliated and secretory cells similar to those in the mammalian lung (Stubbs et al., 2006; Dubaissi and Papalopulu, 2011), and so provide a unique context to study both cellular differentiation and cilia formation, as well as the molecular mechanisms controlling these processes (see Chung et al., 2014). Previously we have used such explant studies to study the role of Sox7 and Sox18 in cardiogenesis (Zhang et al., 2005) and to reveal Snail2/Slug's role in regulating mesodermal induction of neural crest markers (Shi et al., 2011). Using morpholino-mediated down regulation and Cby RNA rescue together with standard and quantitative RT-PCR, *in situ* hybridization, and quantitative confocal microscopy, we have examined the role of Cby in the formation of ciliated cells and cilia, the patterning of the neuroectoderm, the formation and migration of the neural crest, and the regulation of RNA levels of key genes involved in embryonic induction. The results indicate that Cby acts structurally at cilia and as a regulator of a β-catenin/Wnt-signaling feedback loop and has effects on hedgehog signaling pathway components in *X. laevis*.

Results

A search of Xenbase (James-Zorn et al., 2013) using the latest version of the *X. laevis* genome (7.1) revealed the presence of a single *Cby* gene in both *X. laevis* and *Xenopus tropicalis* genomes. In *X. laevis*, but not apparently in *X. tropicalis*, there is a second, much shorter transcript within the first intron of the Cby gene, apparently initiated from a distinct promoter. This transcript, XeXenL6RMv10034349m.g, contains an open reading frame that encodes a 91 amino acid polypeptide; the top hits in a BLAST search revealed a 34% identity to dimethyl-allyltranstransferase and polyprenyl diphosphate synthase from *Streptomyces* sp. CNB091 and

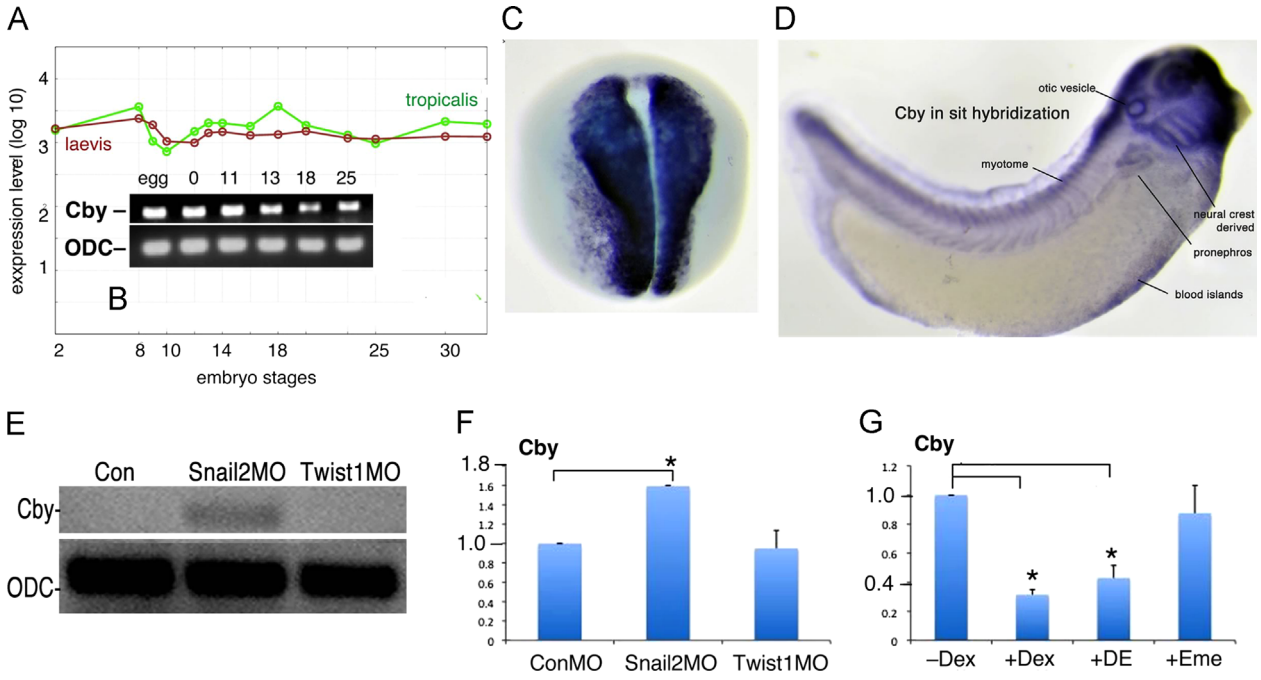

Fig. 1. Cby RNA is supplied maternally and its level remains high throughout early *Xenopus* development (**A**) based on Xenbase data for *X. laevis* (red) and *X. tropicalis* (green); (B) RT-PCR analysis in *X. laevis* of *Cby* RNA at various developmental stages using ornithine decarboxylase (*ODC*) RNA as the normalizing control. *In situ* hybridization studies indicate that *Cby* is expressed at high levels in the neuroectoderm of stage 18 embryos (C); later in embryogenesis (D) Cby is expressed in a range of tissues including the myotome, pronephros, otic vesicle, central nervous system, migrating neural crest, the eye, and blood islands. Standard (E) and qPCR (F) analyses of ectodermal explants derived from control, Snail2/Slug, or Twist1 morpholino (MO) injected embryos revealed an increase in *Cby* RNA in response to inhibition of *Snail2* expression. (G) Ectodermal explants were derived from embryos injected with GR-Snail2 RNA (200 pg/embryo) and either left untreated (–dex) or treated for 2 h with dexamethasone (+dex), dexamethasone and emetine (+dex, +eme), or emetine alone (+eme). *Cby* RNA levels were measured by qPCR with the Y-axis corresponding to the change in Cby RNA level with respect to control condition, either control MO injected (F) or in the absence of dexamethasone (G). Student *t*-test values of <0.05 are indicated by a "*", while a p value <0.01 is indicated by "**" in this and all other figures.

Streptomyces globisporus respectively. Based on its sequence, its translation is not expected to be influenced in any way by the morpholino used to inhibit Cby synthesis (data not shown) and we have not studied the role of this possible transcript further.

Xenbase, using data from Yanai et al. (2011), and our own RT-PCR analyses indicate that *Cby* RNA is supplied maternally and is present at relatively constant global expression levels throughout early development in both *X. laevis* and *X. tropicalis* (Fig. 1A and B). *In situ* hybridization studies revealed that *Cby* RNA is most highly expressed in the neuroectoderm of neurula stage embryos (Fig. 1C) and in a number of tissues in later stage embryos including the myotome, pronephros, otic vesicle, neural crest streams, central nervous system, and blood islands (Fig. 1D). In contrast to other ciliogenesis-associated genes, such as *Rfx2* (Chung et al., 2012), *Cby* RNA does not appear to be present at high levels in the ciliated cells of the epidermis.

We previously reported differences in the ability of mesodermally-expressed Snail2 and Twist1 to induce neural crest in ectoderm (Shi et al., 2011). Our unpublished RNA SEQ analyses in *X. tropicalis* suggested that Cby RNA levels are negatively regulated by Snail2 but not Twist1 (data not shown). We confirmed this observation in *X. laevis* using standard (Fig. 1E) and quantitative RT-PCR (qPCR) (Fig. 1F). To further characterize the regulatory relationship between Snail2 and Cby, we injected embryos with RNA (200 pgs/embryo) encoding a hormone-regulated form of Snail2, GR-Snail2-GFP (Zhang et al., 2006); upon its activation with dexamethasone *Cby* RNA levels decreased. Emetine-mediated inhibition of protein synthesis did not inhibit the Snail2-dependent decrease in *Cby* RNA (Fig. 1G), suggesting that Cby is an "immediate-early", presumably direct target of Snail2 repression.

To define the functional roles of Cby in the early embryo we commissioned GeneTools, LLC to design and synthesize a translation blocking morpholino (Cby MO). We isolated the Cby coding sequence from early embryonic RNA using RT-PCR and constructed two plasmids that encode full length Cby linked in-frame to GFP. The pCS2-Cby-match plasmid encodes an RNA that contains an exact match to the Cby MO sequence, while the pCS2-Cby-GFP-rescue plasmid encodes an RNA in which the region targeted by the Cby MO was altered to reduce complementarity to the morpholino but without changing the final Cby polypeptide sequence (Fig. 2A). Both plasmids were sequenced to confirm the absence of mutations introduced in the process of isolation and subcloning. We tested a rabbit anti-mammalian Chibby antibody (Takemaru et al., 2003) which reacted with Cby-GFP (Fig. 2B) as well as a number of other polypeptides in *X. laevis* (data not shown), which made its use in immunocytochemistry problematic. We confirmed the effectiveness of the Cby MO by injecting fertilized eggs with RNAs encoding GFP or Cby-GFP-match together with either a control or Cby MO (10 ngs/embryo) (Fig. 2B and C). The level of Cby-GFP protein that accumulated was dramatically reduced by the Cby MO but unaffected by the control MO.

Cby is reported to act as an antagonist of β-catenin-mediated Wnt signaling in mammalian cells (Takemaru et al., 2003) but not in *Drosophila* embryos (Enjolras et al., 2012). To determine whether Cby acts as a canonical Wnt pathway antagonist in *X. laevis* we used the β-catenin responsive TOPFLASH reporter system (Korinek et al., 1997). Embryos were injected with TOPFLASH and the control FOPFLASH plasmid DNAs together with RNA encoding ΔG-β-catenin, a mutated form of β-catenin in which the domain responsible for Wnt-regulated stabilization has been removed (Merriam et al., 1997), either alone or together with GFP or Cby-GFP RNAs. We also examined the effect of injecting a control morpholino. These data confirm that over-expression of Cby-GFP inhibits β-catenin-mediated TOPFLASH activation and that MO-induced reduction of Cby levels increased TOPFLASH activity (Fig. 2D), both of which indicate that Cby acts as an intracellular inhibitor of β-catenin mediated Wnt signaling in *X. laevis*.

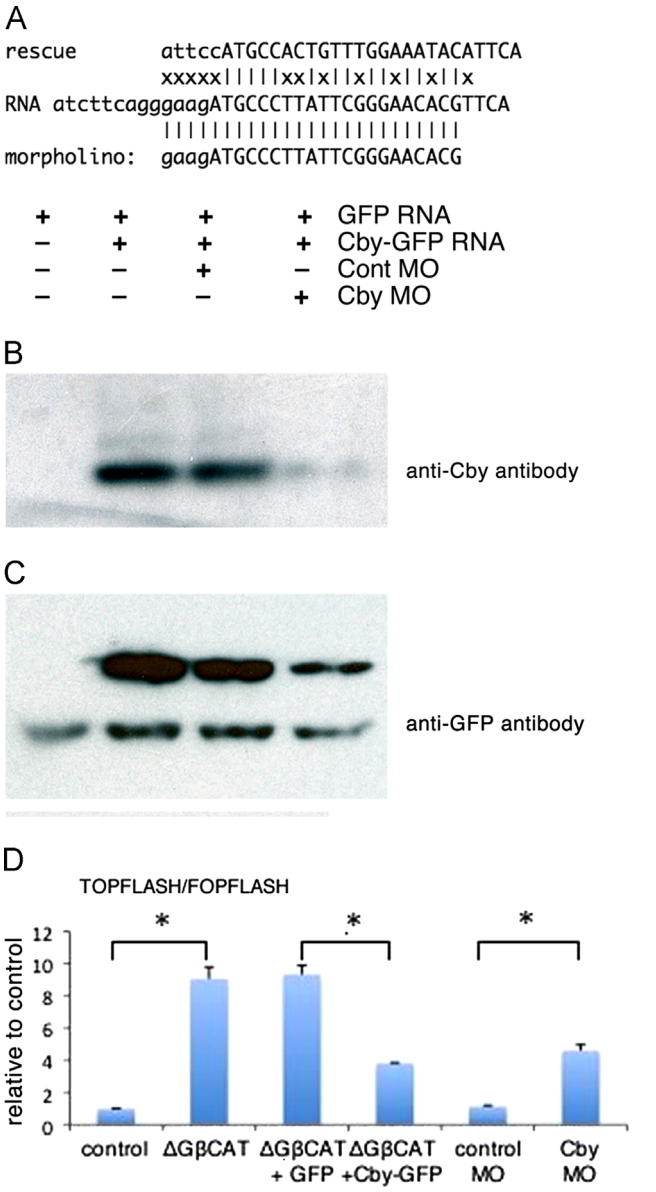

Fig. 2. (A) The Cby MO aligns with the translation start region of the *Cby* RNA; this same sequence is present in the Cby-GFP-match RNA. An alternative, rescuing version of the Cby-GFP RNA, Cby-GFP-rescue, has a number of mismatches in the morpholino-binding region. Immunoblot analysis was carried out using either an anti-rabbit Cby antibody (B) or an anti-GFP antibody (C); embryos were injected with RNAs encoding GFP (200 pgs/embryo) and Cby-GFP match (200 pg/side) and either control or Cby morpholino (10 ngs/embryo) and analyzed at stage 11. Cby MO reduced Cby and Cby-GFP protein levels. In this experiment, the blot was first probed with anti-GFP antibody (C), then stripped and probed with the anti-Cby antibody (B). (D) Embryos were injected with TOPFLASH and FOPFLASH (control) plasmid DNAs (100 pgs/embryo) together with ΔG-β-catenin RNA (100 pgs/embryo) either alone or together with GFP or Cby-GFP (100 pgs/embryo) RNAs or control or Cby morpholinos (10 ngs/embryo). The Y-axis indicates fold increase relative to the control TOPFLASH/FOPFLASH value (set equal to 1). Comparisons between conditions are marked by horizontal bars; in each case, *p*-values were < 0.05.

Cby morphant embryonic phenotypes

Two types of whole embryo morpholino studies were carried out. In "one of two" experiments, one blastomere of a two cell stage embryo was injected equatorially with morpholino (10 ngs/embryo) together with RNA encoding β-galactosidase as a lineage tracer. In "two of two" experiments both cells of two-cell embryos were injected with MO (5+5 ngs/embryo – 10 ngs total). Two of two Cby MO injections produced embryos that were visibly abnormal, smaller, with

a number of defects (compare control Fig. 3A with Cby morphant embryos Fig. 3B). The kink seen in Cby MO embryos was reversed by injection of Cby-GFP-rescue RNA (100+100 pgs/embryo, 200 pgs total (Fig. 3C and D)), but the effect is complicated by the fact that injection of Cby-GFP RNA alone (one of two injection, 200 pgs/embryo) produced rather severe phenotypic effects (Fig. 3E and F). Whole-mount immunocytochemical analyses of Cby morphant embryos revealed defects in the morphology of myotome and heart, but no consistent defect in the normal left-right asymmetry of the heart was noted (data not shown). In one of two injections it was common to find the loss of the pronephros on the injected side; this effect could be rescued by injection of Cby-GFP RNA (Supplemental Fig. S2).

In situ hybridization-based analyses of early neurula stage embryos revealed defects in the expression of the neuroectoderm/central nervous system markers *neural-β-tubulin* (*Tubb2b*), *Engrailed*, and *Krox20* (see Sullivan et al., 2001); these effects were rescued by the injection of Cby-GFP RNA (Fig. 3G–I). Quantitation of the rescue data is presented in Fig. 3J. Similarly, markers of the neural crest, *Twist1* and *Sox9*, were reduced or absent in the Cby morphant region of embryos, but only when higher levels of morpholino, 10 ng/injection (Fig. 4E-F and K, L for *Sox9*, Fig. 4H, I and N, O for *Twist1*) rather than 5 ng/injection (Fig. 4A and B-*Sox9*, Fig. 4C and D-*Twist1*). The loss of Twist1 and Sox9 expression in the 10 ng morpholino-injected blastomeres was rescued by injection of Cby-GFP RNA (Fig. 4G, J, M, and P). Quantitation of these rescue studies is presented in Fig. 4Q. Not surprisingly, we observed gross defects in craniofacial cartilage formation, visualized by Alcian blue staining of Cby morphant embryos (Fig. 4R – control, Fig. 4S – Cby MO, Fig. 4T – Cby MO and Cby-GFP RNA). Transplantation studies, in which the neural crest regions of Cby morphant (5 ngs/embryo)/GFP-expressing embryos were transplanted into the analogous regions of uninjected embryos, revealed that neural crest migration was often aberrant (Fig.4U and V). This effect appears to be due to defects in neural crest migration, because at the 5 ng level of Cby morpholino injection used in these studies the initial expression of neural crest markers was not dramatically altered (see above, Fig. 4A–D).

Effects on ciliated cells

In *Xenopus* the embryonic epidermis becomes speckled with multi-ciliated and secretory cells. The multiciliated cells can be visualized using antibodies against acetylated α-tubulin (AAT) beginning around stage 13 and they are well developed by stage 18; their differentiation begins when the cells are located in subsurface layers (Steinman, 1968; Chu and Klymkowsky, 1989; Stubbs et al., 2006). We analyzed the effects of the Cby morpholino on ciliogenesis in ectodermal explants. Explants have an advantage over intact embryos in that they have a simpler, albeit abnormal developmental fate, since they lack mesodermally and endodermally derive inductive signaling systems (Ariizumi et al., 2009). When blastula-stage animal cap ectoderm is dissected and left intact, it develops into atypical ciliated epidermis with the same general time course as seen in the intact embryo (Jones and Woodland, 1987). Cilia are typically divided into basal body and axonemal regions (Satir and Christensen, 2007). Previous studies localized Cby to the distal end of mother centrioles and the basal body region of cilia (Ishikawa et al., 2005; Steere et al., 2012a). Confocal analyses of ectodermal explants revealed Cby-GFP's

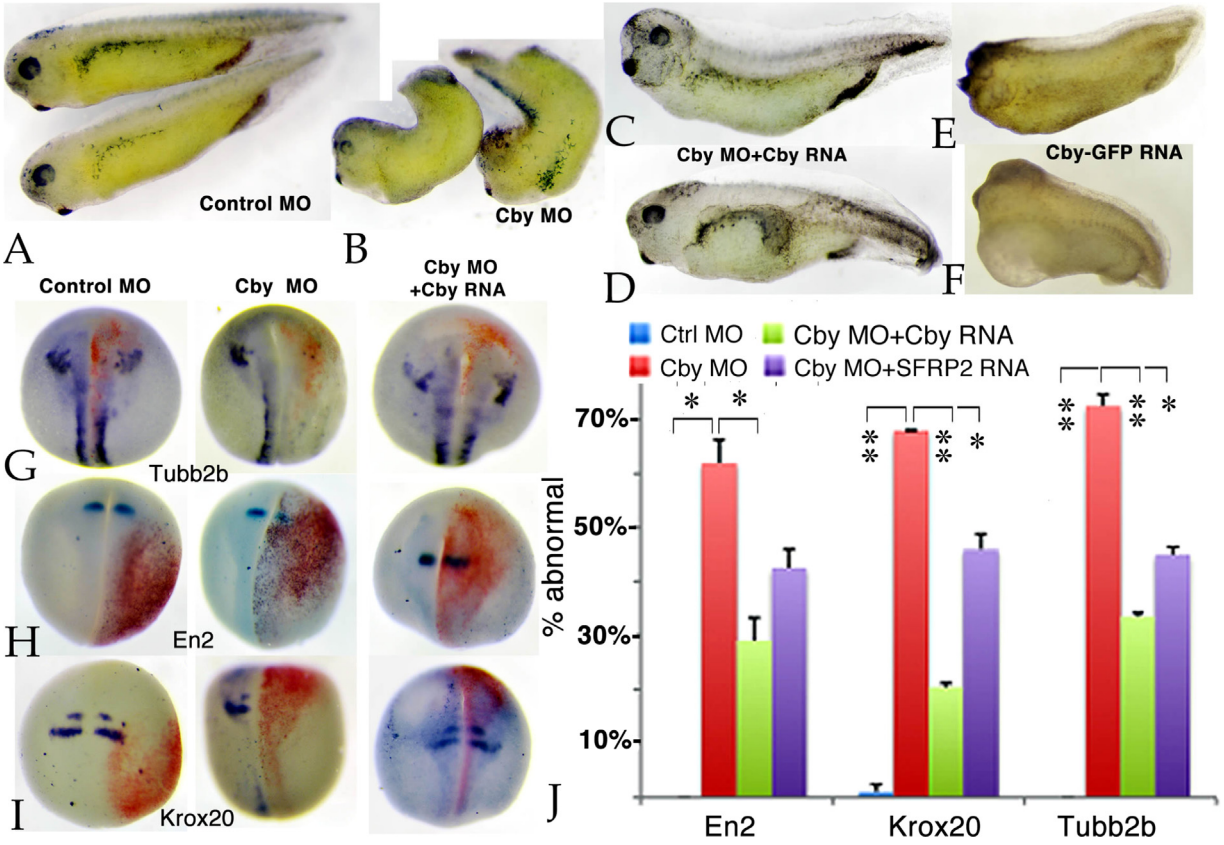

Fig. 3. Compared to uninjected (not shown) or control MO injected embryos (**A**), Cby MO injected embryos typically displayed a noticeable kink (B); injection of Cby-GFP-rescue RNA together with the Cby MO reversed this kink (C and D), while Cby-GFP-rescue RNA alone produced a distinct phenotype (E and F). *In situ* hybridization studies revealed the loss of the neural and patterning markers *Tubb2b* (G), *Engrailed* (H), and *Krox20* (I). These phenotypes were rescued by injection of Cby-GFP-rescue RNA. In panels G–I embryos were injected with either control MO (left panel), Cby MO (center panel), or Cby MO together with Cby-GFP RNA (right panel). All embryos were injected with RNA encoding β-galactosidase as a lineage tracer. Quantitation is provided in panel **J.** Comparisons between conditions are marked by horizontal bars (* for $p < 0.05$ and ** for $p < 0.01$).

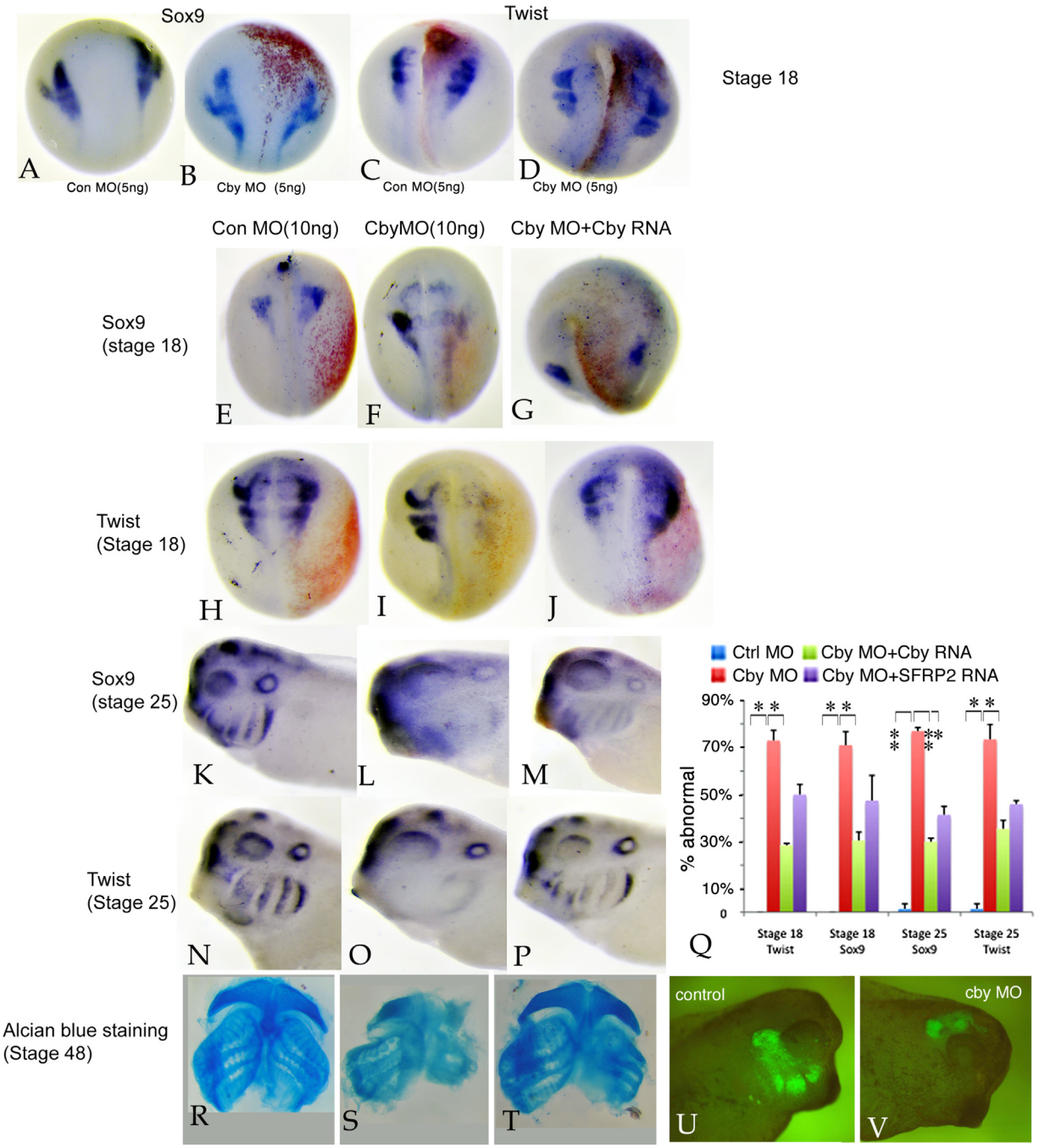

Fig. 4. To examine the effects of morpholino down regulation of Cby, we carried out *in situ* hybridization of embryos injected in one of two blastomeres. Compared to embryos injected with control MO (A and C), injection of 5 ng/blastomere of Cby MO (B and D) had little apparent effect on *Sox9* (A and B) or *Twist1* (C and D) expression. In contrast to control MO injected embryos (E and H), the injection of 10 ngs/blastomere Cby MO (F and I) produced a dramatic reduction in both *Sox9* (E and F) and *Twist1* (H and I). These effects were rescued by the co-injection of Cby-GFP-rescue RNA (200 pg/side) with Cby MO (10 ngs/blastomere)(G – Sox9, J – *Twist1*). A similar effect was seen in later stage embryos; compared to control embryos (K and N), the injection of 10 ngs/blastomere Cby MO (L and O) led to a reduction in Sox9 (K and L) and Twist1 (N and O) expression. This phenotype could be partially rescued by the co-injection of Cby-GFP-rescue RNA (200 pg/side)(M – Sox9, P – *Twist1*). The results from10 ngs/blastomere injection experiments are quantified in part **Q** with p-values (* for $p < 0.05$ and ** for $p < 0.01$). Alcian Blue staining revealed defects in Cby MO (10 ngs/blastomere) injected embryos (S) compared to control (R) embryos; these defects were ameliorated by co-injection of Cby-GFP-rescue RNA (**V**). Neural crest transplants from GFP injected embryos migrate normally (U) while the analogous region from Cby morphant embryos (5 ngs/embryo) failed to migrate (V).

localization to the basal body region of cilia in multi-ciliated cells, as determined by a comparison to centrin and AAT localization (Fig. 5A–C). While nuclear localization sequences have been reported to be present in Cby (Li et al., 2010), we did not observe any obvious nuclear accumulation of the Cby-GFP protein, although in cells expressing high levels of the protein, it was found associated with the plasma membrane (not shown). The lack of nuclear localization may be due, at least in part, to the fact that Cby-GFP is thought to cooperate with other proteins to move β-catenin out of the nucleus and into the cytoplasm (Takemaru et al., 2003; Li et al., 2010; Mancini et al., 2013) and perhaps reflects the effects of the expression of the Cby-interacting protein TC1(C8orf4) (Jung et al., 2006), whose RNA levels (according to Xenbase) increase following the mid-blastula transition (Supplemental Fig. S4).

Using ectodermal explants we characterized the effects of Cby MO injection on the formation of ciliated cells, which are interspersed with non-ciliated cells, and the number of cilia per ciliated

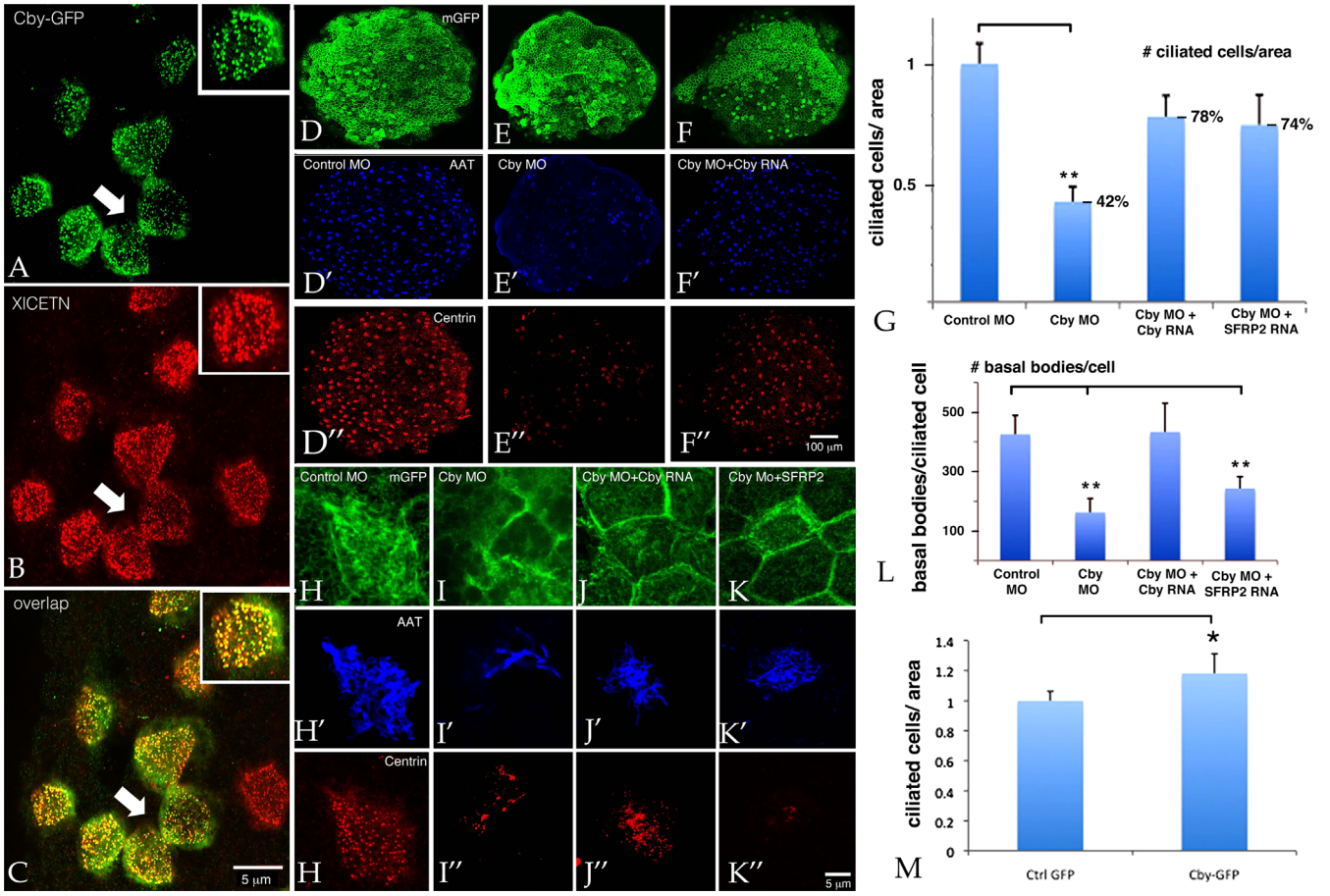

Fig. 5. To characterize the intracellular localization of Cby-GFP, both blastomeres of two-cell stage embryos were injected with Cby-GFP RNA (200 pg/embryo). Ectodermal explants were isolated at stage 9 and fixed at stage 18. Confocal images were taken at 40X magnification. Immunofluorescence staining was performed with an chicken anti-GFP antibody (**A**) and a rabbit anti-*X. laevis* Centrin antibody (B), (C) is the merged image of (A) and (B), insets in each panel show higher magnification view. In explants from Cby-GFP RNA injected embryos, we did find juxtaposed ciliated cells (arrows)(see below – part M). At higher injected RNA levels, Cby-GFP can also be seen associated with membranes. To examine the effects of reducing Cby levels on the frequency of ciliated cells (D–G) and the number of basal bodies per ciliated cell (H–L) both blastomeres of two-cell embryos were injected with membrane-GFP RNA together with either control MO (D, D′, D″ and H, H′, H″), Cby MO (E, E′, E″ and I, I′, I″), Cby MO plus Cby-GFP RNA (F, F′, F″ and J, J′,J″), or Cby MO plus SFRP2 RNA (K, K′, K″), Membrane-GFP (D–K) was visualized using an anti-GFP antibody, while anti-AAT (D′–K′) and anti-centrin (D″–K″) antibodies were used to visualized ciliated cells and basal bodies, respectively. Confocal images were taken at 10 × magnification. Quantitation of the Cby morpholino's effect on the number of ciliated cells per cap (G) (*y*-axis corresponds to number of cilia per area, normalized to control morphant explants) and the number of basal bodies per cell (***L***) are shown. Injection of Cby-GFP RNA (M) led to an increase in the number of ciliated cell per unit area in ectodermal explants. Comparisons between conditions are marked by horizontal bars (* for $p < 0.05$ and ** for $p < 0.01$).

cell. Results were quantified using a semi-automated script through ImageJ (see Supplemental Fig. S3) and showed that the density of ciliated cells (ciliated cells per unit area) (Fig. 5D, D′, and D″ – control and Fig. 5E, E′, and E″ – Cby morphant) and the number of centrin-stained basal bodies per ciliated cell (Fig. 5H, H′, and H″ – control and Fig. 5I, I′, and I″– Cby morphant) were reduced in Cby morphants. Both phenotypes could be rescued by the injection of RNA encoding the Cby-GFP-rescue construct (Fig. 5F, F′, and F″ – ciliated cells per unit area and Fig. 5J, J′, and J″ – cilia per ciliated cell). Quantitation of these effects is presented in Fig. 5G and L. In the course of these rescue studies, we noticed that injection of Cby-GFP RNA led to cases in which multiciliated cells were located next to one another (see arrows Fig. 5A and C), a situation that is observed, but only rarely in control explants and embryos (see Chu and Klymkowsky, 1989; Stubbs et al., 2006). Quantitative analyses (Fig. 5M) indicates a small, but statistically significant increase in multiciliated cells per unit area in Cby-GFP compared to control RNA explants.

The number of primary cilia present in cells in the neural tube at stage 26 was found to be reduced in Cby MO morphants (Fig. 6A and B). This decrease in primary cilia was rescued by injection of Cby-GFP RNA (Fig. 6C). In contrast, we found no dramatic effect on the number of gastrocoele roof plate cilia in Cby morphant embryos (Fig. 6D and E). We have yet to be able to visualize any association of Cby-GFP with either gastrocoele roof plate cilia (motile) or primary, that is, immotile cilia; Cby-GFP was localized through the cytoplasm in sections of neural tube taken at stage 26 (Fig. 6F–H). Interestingly, we also failed to find centrin (visualized with an anti-Xenopus centrin antibody) localized to the basal body region of neural tube primary cilia; instead centrin staining was concentrated in nuclei (Fig. 6I), perhaps not surprising since it has been reported that most of a cell's centrin is located within the nucleus (Paoletti et al., 1996).

Molecular studies

While analyzing Cby morphant embryos, we noted the loss of *Tubb2b* expression in neural ectoderm as monitored by *in situ* hybridization (Fig. 3G) and by RT-PCR (see below). This led us to explore changes in gene expression in control and morphant ectodermal explants more generally, exploiting their developmental simplicity (see above). Fertilized eggs were injected at the one cell stage with either control or Cby morpholino (10 ngs/embryo) and RNA (150 pgs/embryo) encoding a membrane bound form of GFP, GFP-CAAX. At the mid blastula stage (stage 8/9) the animal pole ectodermal region was dissected, allowed to heal and then cultured

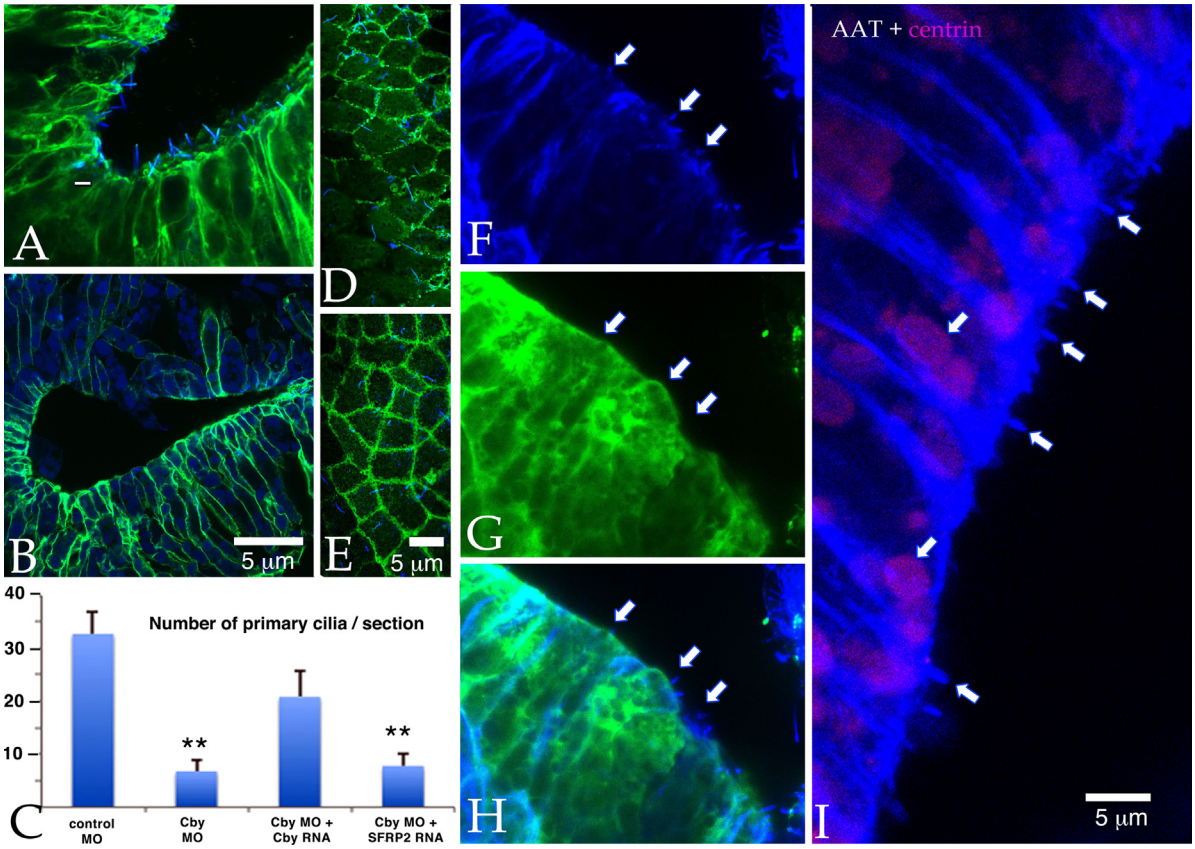

Fig. 6. Both blastomeres of two cell stage embryos were injected with either control (A and D) or Cby (B and E) morpholino (10 ngs/embryo) and membrane-GFP RNA. The neural tube region of stage 26 embryos (A and B) and the gastrocoele roof plate regions of stage 19 embryos (D and E) were dissected and stained for injected membrane-GFP (green) and AAT (blue). Primary cilia were absent or greatly reduced in Cby morphant neural tubes (A and B). (C) To quantitate the effect of the Cby morpholino on primary cilia formation, and the ability of Cby-GFP or SFRP2 RNAs to rescue this effect, 7–10 GFP positive embryos for each group were analyzed. For each embryo, a series of sections were generated and 5 representative images (taken at 40X) were selected and use to calculate mean number of cilia. "**" indicates a p value < 0.01 compared to control embryos. In contrast to the effect on primary cilia, gastrocoele roof plate cilia were present in Cby morphant gastrocoele roof plate tissue (D and E). In experiments in which fertilized eggs were injected with Cby-GFP; at stage 25 embryos were fixed, sectioned and stained for AAT (F) or GFP (G); (H) is the overlap of (F) and (G). While cilia are visible (arrows) GFP staining, presumably associated with CbyGFP is not concentrated there. When similar sections from uninjected embryos were stained for centrin (I – magenta) and AAT (blue), centrin was found localized to nuclei (arrows pointing down) but not to the basal body regions of primary cilia (arrows pointing up). Scale bars in part B, E, and I marks 5 μm for parts A and B, D and E, and F–I respectively.

until sibling embryos had reached stage 18. *In situ* studies revealed that the level of expression of *Tubb2b* RNA was reduced in Cby morphant explants, a decrease that was rescued by the co-injection of Cby-GFP-rescue RNA (Fig. 7A–C). Based on their well known role in embryonic patterning, we examined the levels of *BMP4*, *FGF8*, *Noggin*, *Wnt8a*, as well as *Tubb2b* RNAs in control and Cby morphant ectodermal explants by standard (Fig. 7D) and quantitative RT-PCR (Fig. 7E). Levels of *BMP4*, *Noggin*, and *Tubb2b* RNAs decreased in Cby morphant explants compared to controls, while the level of *Wnt8a* RNA increased while the level of *FGF8* RNA was unaltered.

Chung et al. (2014) recently published an analysis of the transcription factor network involved in the specification of epidermal multiciliated cells in *X. laevis* ectoderm. Given the effect of Cby morpholino on the number of multiciliated cells per unit area in ectoderm explants, we examined the levels of RNAs for genes implicated in the regulation of multiciliated cells formation including *Foxj1a*, *Myb*, *Rfx*, and *Multicilin*; we found no effect on the levels of these RNAs by either standard (Fig. 7F displays the results of two duplicate experiments for *Multicilin*) or quantitative RT-PCR (Fig. 7G). Similarly, we found no significant changes in the levels of *Notch* or *Delta* RNAs (data not shown).

We repeated such studies in whole embryos, injected in both blastomeres of the two-cell stage with a total of 10 ngs of control or Cby morpholino and analyzed these embryos at stage 11. This is a time point earlier than that used in ectodermal explants and was chosen to limit as much as possible the cascade of inductive effects that occur during gastrulation and neurulation. As in the case of ectodermal explants, we observed an increase in *Wnt8a* RNA and a decrease in *BMP4* and *Tubb2b* RNAs but no effect on *Noggin* (Fig. 8A). We also found a reproducible decrease in the levels of RNAs encoding the Hedgehog pathway associated *Gli2*, *Gli3*, and *Shh* proteins (Fig. 8B).

Given Cby's role as an antagonist of β-catenin-mediated Wnt signaling (Fig. 2C) (Takemaru et al., 2003; Steere et al., 2012a) and the observed increase in *Wnt8a* RNA levels in Cby morphant explants and embryos, we examined whether these changes in RNA levels were secondary "feedback" effects associated with increased canonical Wnt signaling. Embryos were injected with control or Cby morpholinos, RNA encoding membrane-bound GFP, and RNA encoding either Dkk1 (Glinka et al., 1998) or SFRP2 (Bradley et al., 2000), two mechanistically distinct inhibitors of canonical Wnt signaling. The striking result was that the inhibition of Wnt mediated signaling largely reversed the effects of the Cby morpholino on *Wnt8a*, *BMP4*, *Noggin*, and *Tubb2b* RNA levels in ectodermal explants (Fig. 7E and F) and *Wnt8a*, *BMP4*, and *Tubb2b* RNAs in whole embryos (Fig. 8A). *SFRP2* RNA injection did not reverse the Cby morpholino's effects on *Gli2*, *Gli3*, or *Shh* RNA levels (Fig. 8B). Expressing SFRP2 in Cby morphant explants increased the density of ciliated cells (Fig. 5G) but not the number of cilia per cell (Fig. 5K, K′,K″ and L). We found that the injection of *SFRP2* RNA

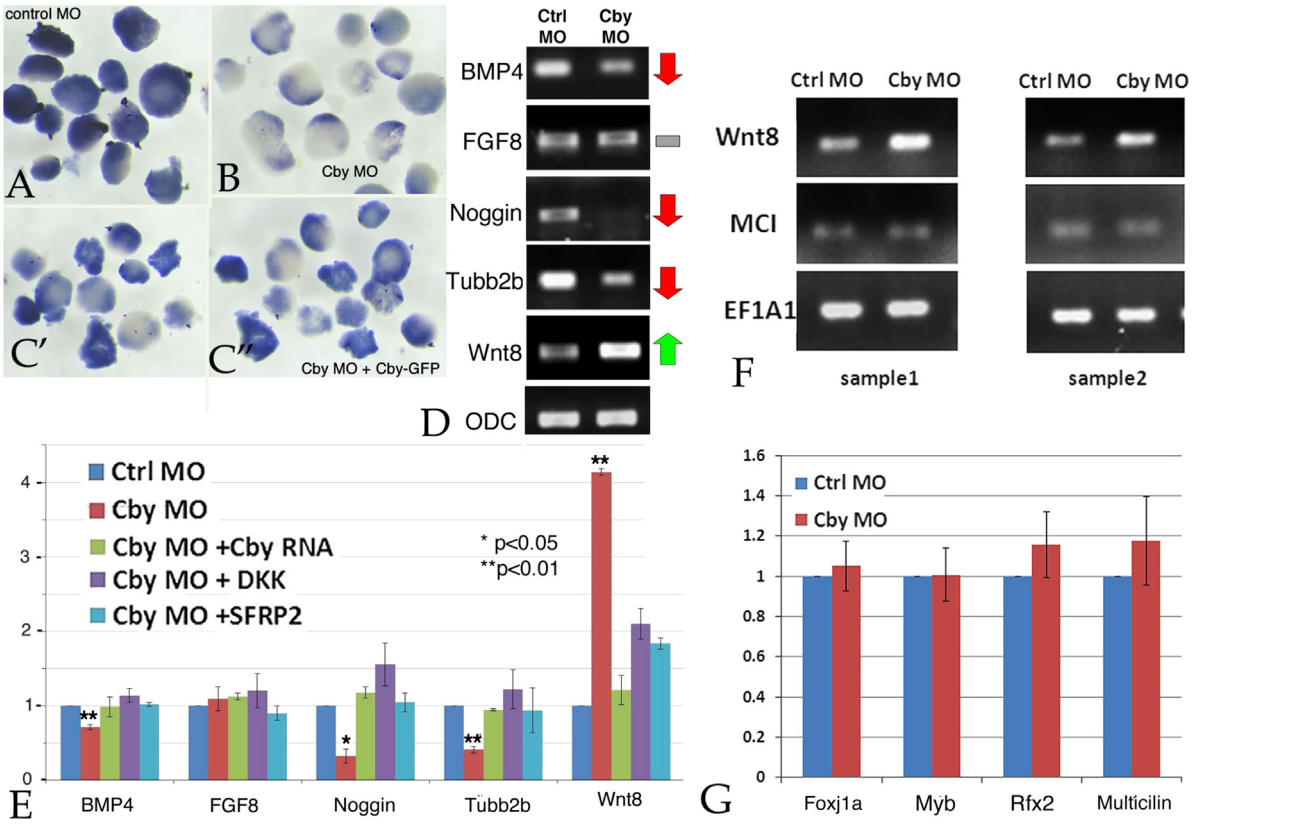

Fig. 7. Ectodermal explants derived from control (A) or Cby (B) morpholino injected embryos were stained *in situ* for *Tubb2b* RNA; co-injection of RNA encoding Cby-GFP-rescue (C′ and C″) increased the level of *Tubb2b* RNA staining. (D) Control (Ctrl MO) and Cby MO explants were analyzed at stage 18 using RT-PCR; Cby morphant explants displayed decreased levels of *BMP4*, *Noggin*, and *Tubb2b* RNAs, and increased levels of *Wnt8a* RNA. Levels of *FGF8* RNA were unchanged. (E) qPCR analyses of control and Cby morphant explants co-injected with Cby-GFP-rescue, *Dkk1*, or *SRFP2* RNAs. Both Cby-GFP and the two Wnt signaling inhibitors returned all RNAs to control levels. Standard (F) and qPCR (G) analyses of control (Ctrl) and Cby morphant ectodermal explants, analyzed at stage 18, revealed a no change in the levels of the ciliogenesis associated transcription factors *Multicilin* (F and G), *Foxjia*, *Myb*, and *Rfx2* (G).

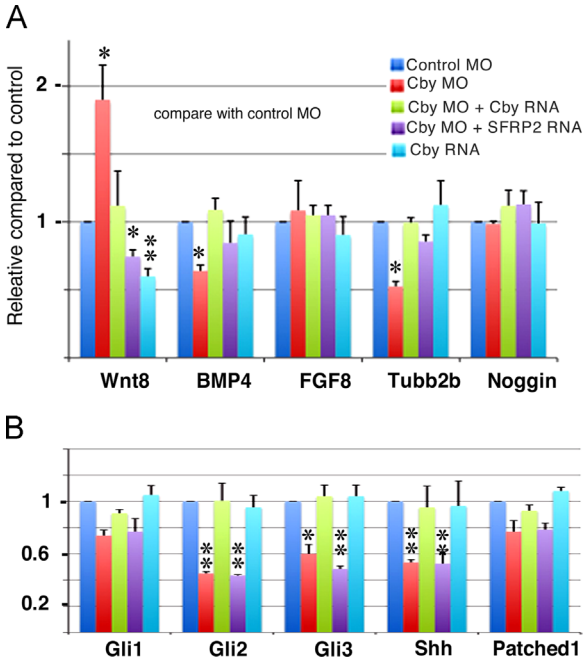

Fig. 8. Each blastomere of a two cell embryo was injected with either Control or Cby morpholino (10 ngs/embryo total) together with RNA encoding membrane-bound GFP. In rescue studies, embryos were also injected with RNAs (200 pgs/embryo total) encoding either Cby-GFP-rescue or SFRP2. Embryos were analyzed at stage 11 by qPCR. Panel A displays the results for *Wnt8a*, *BMP4*, *FGF8*, *Tubb2b*, and *Noggin*, panel B displays the results for *Gli1*, *Gli2*, *Gli3*, *Shh*, and *Patched* RNAs. This experiment was carried out two independent times with similar results.

could partially rescue the phenotypic effects of the Cby morpholino on neural tube patterning (Fig. 3J) and neural crest marker expression (Fig. 4Q). The late stage phenotypic rescue effects of *SFRP2* RNA injection were somewhat less dramatic than those observed in Cby-GFP RNA rescued Cby morphant embryos. It is not clear whether this "rescue" is due solely to SFRP2-mediated inhibition of Cby's effects on Wnt signaling or involves other effects associated with SFRP2 over-expression; distinguishing between these two alternatives is beyond the resolution of our experimental approach. We have summarized the molecular interactions and the effects of various perturbations in Fig. 9, which is discussed in greater detail below.

Discussion

That different, even related organisms use distinct mechanisms in their early developmental pathways is perhaps not as well appreciated as it might be. For example, Nanog, a NKL-family homeodomain-containing transcription factor that plays a conserved and critical role in early embryonic patterning and the regulation of differentiation (see Okita et al., 2007 and references therein) is apparently missing altogether from both *X. laevis* and *X. tropicalis* genomes (Scerbo et al., 2012). Since a functionally similar Nanog homolog is present in axolotl (Dixon et al., 2010), we can assume that various adaptations at the molecular and cellular level have occurred in the *Xenopus* lineage to compensate for its absence (see Scerbo et al., 2012). Similarly Snail2, which appears to directly regulate *Cby* expression (Fig. 1E–G), plays an essential role in mesoderm and neural

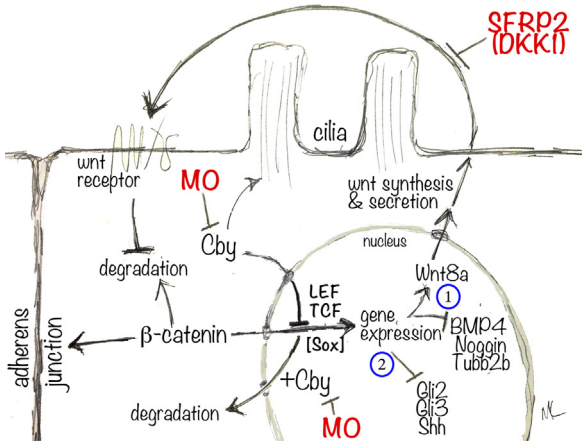

Fig. 9. This cartoon summarizes our observations and integrates them into the context of previous studies. Cby is associated with the basal body region of the cilia of multiciliated cells. The Cby morpholino ("MO" in red) down regulates Cby protein levels, leading to a reduction in both the number of cilia per cell and the density of multiciliated cells in ectodermal explants; both phenotypes were rescued by the injection of Cby-GFP RNA. Cby inhibits the effects of β-catenin on gene expression, as reflected by the effects of both *Cby* RNA and MO on the activity of the β-catenin-responsive TOPFLASH reporter. Cby is thought to act on gene expression primarily by driving β-catenin out of the nucleus. In the context of the canonical (β-catenin-dependent) Wnt signaling pathway, this inhibits the interaction between β-catenin and LEF/TCF HMG-box type transcription factors involved in gene activation. We note that β-catenin also interacts with other transcription factors, including a subset of Sox type HMG box transcription factors, so the exact details of the Cby MO's effects on gene expression in any particular cell type remain to be resolved. We have identified two distinct patterns of altered RNA levels in Cby morphant explants. In the first (indicated by blue circled 1), there is a increase in *Wnt8a* RNA levels and a decrease in *BMP4*, *Noggin*, and *Tubb2b* RNAs. These changes are largely blocked by expression (from injected RNA) of the secreted Wnt inhibitors SFRP2 and DKK1 (in red). This suggests that these effects are dependent upon a feed-forward Wnt signaling loop, which may be autocrine, juxtacrine, or both. SFRP2 also at least partially reverses the *Cby* morpholino's effects on multiciliated cell density in explants and neuroectodermal and neural crest marker expression in embryos, again suggesting that the *Cby* morphant phenotype is due, at least in part, to enhanced Wnt-signaling effects. Cby MO effects on *Gli2*, *Gli3*, and *Shh* RNA levels (indicated by blue circled 2) are not blocked by SFRP2, and so appear to be direct effects of decreasing Cby levels and not mediated by downstream Wnt signaling. SFRP2 does not reverse Cby MO's effects on cilia number in multiciliated cells or the neural tube, suggesting that these effects involve distinct Cby-regulated processes.

crest development in *X. laevis* (Carl et al., 1999; Mayor et al., 2000; Shi et al., 2011). In contrast, in the mouse Snail1 plays an early embryonic role, whereas neither Snail1 nor Snail2 appeared to be required for neural crest formation (Murray and Gridley, 2006). It is the combination of these lineage specific adaptations that makes *Xenopus* a useful context within which to reveal aspects of gene function that are hidden or compensated for in other organisms or tissues. In the case of Cby, it is presumably just these features that underlie the drastic effects of Cby down-regulation in *Xenopus* compared to the superficially less dramatic, post-natal phenotype described in the mouse (Voronina et al., 2009).

The use of ectodermal explants (animal caps) and whole embryo studies enable us to directly examine the effect of morpholino-mediated decrease in Cby protein on ciliated cell formation, cilia assembly, and changes in gene expression. We have summarized these observations in a schematic form in Fig. 9. A number of questions emerge from these observations and the observations of others. These include how the cytoplasmic/nuclear *versus* cilia-associated levels of Cby protein are regulated. It is worth noting that a number of the proteins previously reported to interact with Cby, including ODF2/Cenexin1, C8orf4, Rab8a, a number of 14-3-3 proteins, and Clusterin are expressed (at least in terms of RNA) in early *Xenopus* embryos (see supplemental Fig. 4). The ability of the secreted Wnt inhibitor SFRP2 to return the density of multiciliated cells and the levels of *Wnt8a*, *BMP4*, *Noggin*, and *Tubb2b* RNAs to near normal levels suggests that an autocrine (and perhaps paracrine) Wnt signaling feedback loop, blocked by SFRP2, is involved in these effects. The ability of SFRP2 to at least partially ameliorate later stage neural tube and neural crest phenotypes suggests that this loop may also be important in later stage Cby morphant phenotypes.

The Cby morpholino's effects on the RNA levels of some Hedgehog signaling pathway components in whole (stage 11) embryos was surprising, since embryos at this stage are not known to have primary cilia (Steinman, 1968), thought to mediate Hedgehog signaling. That said, an analysis of Hedgehog pathway RNAs (Supplemental Fig. S4) indicates that all of these components are expressed in the embryo, at least as RNAs, at stage 11. The observation that the effects of Cby on *Gli2*, *Gli3*, and *Shh* RNAs are not altered by SFRP2 suggests that their regulation involves a distinct, non-Wnt signaling pathway. This pathway may involve cilia or cilia-associated systems, since SFRP2 also fails to rescue the effects of the Cby morpholino on the number of cilia per cell in multiciliated ectodermal cells or the presence of primary cilia in the neural tube (see Fig. 6C).

Up to now the focus on Cby's regulatory roles has been primarily as a regulator of β-catenin-mediated Wnt signaling, it is likely that the network of interactions involving Cby is likely to be complex. A number of proteins are structurally similar to β-catenin; these include plakoglobin (ɣ-catenin) and the nuclear importins (see Klymkowsky, 2005). Plakoglobin, for example, can accumulate in nuclei (Karnovsky and Klymkowsky, 1995) and nuclear plakoglobin has been implicated in the differentiation of cardiac progenitor cells into adipocytes (Lombardi et al., 2011). Whether Cby interacts with and influences the behavior of other β-catenin-like proteins remains unexamined.

In addition, Cby's effect on β-catenin may go beyond canonical Wnt signaling. Over-expression of Cby has been reported to generate an unfolded protein response in BCR-ABL1$^+$ cells (Mancini et al., 2013); whether it has similar effects in other cell types, such as those of the early embryo, is unclear. On the other hand, the absence of Cby could effect β-catenin levels and/or its intracellular distribution, which in turn could influence the activities of other β-catenin-interacting proteins (see Kormish et al., 2010). For example, a number of Sox-type HMG-box transcription factors interact with β-catenin (Zorn et al., 1999; Zhang et al., 2003; Sinner et al., 2004; Ye et al., 2014). In addition β-catenin has been reported to interact with centrosomal proteins and dyneins (Ligon et al., 2001; Mbom et al., 2013), although the physiological significance of these interactions remains to be elucidated.

As a beginning step toward the dissection of these regulatory interactions, we have begun a high resolution ultrastructural and molecular analyses of the effects manipulating levels of Cby on ciliary ultrastructure, cellular organization, and gene expression, as well as attempting to use the Cby-GFP chimeric protein to isolate and analyze Cby-associated proteins using immunoprecipitation and mass spectroscopy. Only such a coordinated global analysis is likely to resolve the network of Cby's complex structural and regulatory interactions.

Materials and methods

Embryos, their manipulation and analysis

X. laevis embryos were staged, and explants were generated, following standard procedures (Nieuwkoop and Faber, 1967; Sive et al., 2000; Shi et al., 2011). Capped mRNAs were transcribed from linearized plasmid templates using mMessage mMachine kits (Ambion) following manufacturer's instructions. At the two-cell stage embryo injections were directed equatorially; for explant

studies injections were targeted to the animal hemisphere region. As an injection tracer, we routinely included RNAs (150 pgs/embryo) encoding either β-galactosidase, green fluorescent protein (GFP) or GFP-CAAX, which is membrane-associated. In the case of GFP/GFP-CAAX RNA injection, embryos were examined at stage 10–11 by fluorescent microscopy to confirm the accuracy of injection. Animal caps were isolated from stage 8–9 blastula embryos in 0.5 MMR (Sive et al., 2000; Shi et al., 2011), transferred into wells on an 2% agarose coated plate and harvested when siblings reached stage 18. Neural crest explants were carried out as described previously (Carl et al., 1999). RNA isolation, RT-PCR and qPCR analyses were carried out as described previously (Zhang et al., 2003, 2006). cDNA synthesis was performed using 1 μg purified RNA and a Verso cDNA kit (Thermo Scientific) following manufacturer's instructions. Real-time (quantitative) PCR was carried out using a Mastercycler Epgradient Realplex device (Eppendorf). PCR reactions were set up using DyNAmo SYBR Green qPCR kits (Finnzymes). Each sample was normalized to the expression level of ornithine decarboxylase (ODC). The cycling conditions used were 95 °C for 5 min; then 40 cycles of 95 °C for 15 s, 56 °C for 15 s, 60 °C for 30 s. The ΔΔCT method was used to calculate real-time PCR results. The primers used for RT-PCR analysis were Ornithine decarboxylase (ODC) [U 5′-CAG CTA GCT GTG GTG TGG-3′ D 5′-CAA CAT GGA AAC TCA CAC-3′]; Wnt8a [U 5′-TGA TGC CTT CAC TTC TGT GG-3′ D 5′-TCC TGC AGC TTC TTC TCT CC-3′]; BMP4 [U 5′-TGG TGG ATT AGT CTC GTG TCC-3′ D 5′-TCA ACC TCA GCA GCA TTC C-3′]; Noggin [U 5′-AGT TGC AGA TGT GGC TCT-3′ D 5′-AGT CCA AGA GTC TCA GCA-3′]; FGF8 [U 5′-TGG TGA CCG ACC AAC TAA GC D 5′-CGA TTA ACT TGG CGT GTG G]; TUBB2B [U 5′-CCA GGC TTT GCC CCA TTA AC D 5′-GCT ACT GTG AGG TAG CGT CC]; Shh [U 5′-GTA TTG GCC TCC TGC TAT GC D 5′-AGG TCA ACT TGG TGG TGA GG]; Gli1 [U 5′-GTG GAT CAG CCA TCT CTT CC D 5′-TGG CAC TGC TTG AAT ATC TCC]; Gli2 [U 5′-GCA CTA CAA TCG CTC TGA CG D 5′-AGC ATG AGG TCA TCG TCT CC]; Gli3 [U 5′-CAG TCG AAG ATC CAG TGA GG D 5′-TTC AGC CTG TAT TGC TGT GC]; Patched-1 [U 5′-GCA GAC GAT AGG CCT GAG AC D 5′-AGC CTC CAC AAA GTC GGAT G]; Smoothened [U 5′-TGG ATA CGT GCA AGA AGA CC D 5′-CAA CAA CGT GGA GCA TTC C]; Notch [U 5′ACT GGA CAG GCC AAT ACT GC D 5′ GTC CAG CCG TTG ACA CAA AC]; Delta [U 5′ CCA GAC TCT GCC TAC TCA ACG D 5′ CAC CTC TGT TGC AAT GAT GC]; Foxj1 [U 5′-GCA CCC ATG GGA AGA GAA CA D 5′-CTG CCG GAA ATG CCT CAT TG]; Rfx2 [U 5′-CTG TTG CGC TTA GGA CAT CG D 5′-TGG ACA GTC TGG ACC TGT TG]; Myb [U 5′-CGA TTC GTG CCT AGG AGA CC D 5′-AAA GTA CCG GGC TGG TGA TG]; and Multicilin [U 5′-TCT CAT GCA GCC CAG TCT TG D 5′-TTG CAG GGG GTT GGT CAT AC].

Morpholinos and plasmids

The Cby morpholino (5′ CGTGTTCCCGAATAAGGGCATCTTC 3′) was designed by and purchased from Gene Tools, Inc. Control, Snail2/Slug and Twist1 morpholinos have been described previously (Zhang et al., 2006; Zhang and Klymkowsky, 2009). We generated plasmids that encode Cby-GFP chimeras that either perfectly match (pCS2-Cby-GFP-match) or maximally mismatch (pCS2-Cby-GFP-rescue) the Cby morpholino (see Fig. 2A). Other plasmids used those that encode membrane-bound GFP, GFP-CAAX, supplied by Kristen Kwan (U. Utah), ΔG-β-catenin (Merriam et al., 1997), Dickkopf-1 (Glinka et al., 1998), SFRP2 (Bradley et al., 2000), and GR-Slug/Snail2 (Zhang et al., 2006). The details of the TOPFLASH/FOPFLASH assay have been described previously (Zhang et al., 2006). Statistical analysis were based on values expressed as mean ± standard deviation. Comparisons between Cby MO alone or together with rescue RNA *versus* control MO were analyzed by unpaired student's *t*-test. $p < 0.05$ was considered as significant in all analyses.

Immunoblot and in situ hybridization studies

For *in situ* hybridization studies, anti-sense probes for *Sox9*, *Twist1*, *Krox20*, *En2*, and *Tubb2b* RNAs were synthesized using digoxigenin-UTP following standard methods. Generally embryos were co-injected with β-galactosidase RNA (50 pg/embryo) and β-galactosidase activity was visualized in fixed embryos using a brief Red-Gal (Research Organics) reaction.

Immunocytochemistry

Whole-mount immunocytochemistry was carried as described by Dent et al. (1989). To image gastrocoele roof plate cilia or primary cilia in the neural tube, control or Cby morpholino (together with RNA encoding membrane-bound GFP as a lineage tracer) were injected alone or together with rescuing RNAs into dorsal blastomeres at the 4-cell stage. To examine gastrocoele roof plate cilia cilia, gastrocoel roof plates were dissected from stage 19 embryos and fixed in MEMFA and prepared for immunohistochemistry as described by Chung et al. (2012). To examine neural tube primary cilia, embryos at stage 26 were fixed in MEMFA and embedded in 2–4% low melting agarose and either 50 μm or 300 μm sections were generated using a Leica VT1000S Vibratome. Images were collected using a Zeiss 510 Confocal Laser Scanning Microscope. The mouse monoclonal anti-acetylated α-tubulin (AAT) antibody 6-B-11 was used to visualized ciliated cells (Chu and Klymkowsky 1989), pronephros was visualized using the mouse monoclonal antibody 4A6 (Vize et al., 1995) obtained from the Developmental Studies Hybridoma Bank, and skeletal muscle and heart were visualized using the mouse monoclonal anti-sarcomeric tropomyosin (T9283) (Cary and Klymkowsky, 1994; Cary and Klymkowsky, 1995), purchased from Sigma. Rabbit anti-Xenopus centrin was supplied by Sergei Sokol (Kim et al., 2012). A rabbit anti-mouse Cby antibody was generously supplied by Feng-Qian Li (Takemaru et al., 2003) and tested in whole-mount on Xenopus embryos. Immunoperoxidase stained embryos were bleached before staining, while immunofluorescence embryos were not. *In situ* hybridization images were captured using a Nikon D5000 camera on a Wild microscope. Images were manipulated with Fireworks CS6 software (Adobe) using “auto levels” and “curves” functions only. Immunoblot analysis was carried out as described previously in Zhang et al. (2003) using an rabbit anti-Chibby or anti-GFP antibody, for immunocytochemistry, a chicken anti-GFP antibody was used (Immunology Consultants Lab, Inc.).

Confocal microscopy and automated quantification

We developed two automated image processing algorithms implemented using the ImageJ macro scripting language. The algorithms were optimized using our antibody staining and confocal acquisition settings to reliably segment image features in a semi-automated fashion and utilized the FeatureJ suite of plugins developed and distributed by Erik Meijering (University Medical Center Rotterdam).[2] The first algorithm was designed to quantify ciliated cell numbers per unit area in ectodermal explants imaged with a 10× objective (0.3 N.A.) at a resolution of 1024 × 1024 pixels (pixel size 1.24 μm) in which explants comprised approximately 25% of the image area. In order to segment the ectodermal explant, the GFP image was convolved with a Gaussian kernel (smoothing radius of 5 pixels) and the image was thresholded to the mean pixel intensity of the entire image. To segment ciliated cells within the explant, the acetylated α-tubulin (AAT) image was

[2] http://www.imagescience.org/meijering/software/featurej/.

convolved with a Laplacian of Gaussian kernel (smoothing radius of 3 pixels). The resulting 32-bit image was inverted and the image was thresholded to the mean pixel intensity plus a single standard deviation and all structures with an area greater than 50 pixels were considered to be ciliated cells. To determine the fraction of the animal cap that contained ciliated cells, the total area of all individual ciliated cells was summed and divided by the area of the animal cap.

The second algorithm was designed to quantify basal body numbers within individual ciliated cells imaged using a 100× objective (1.4 N.A.) at a resolution of 1024×1024 pixels (pixel size 88 nm). A single ciliated cell typically comprised approximately 25% of the image area. To segment the ciliated cell, the contrast of the 16-bit AAT channel was enhanced to achieve 0.005% pixel saturation before being converted to 8-bits. Next, the image stack was convolved with a Gaussian kernel in the XY dimension (smoothing radius of 10 pixels) and a maximum intensity Z projection (MIP) of the image was created. The MIP was then thresholded using Huang's threshold and the threshold value was applied to the Gaussian smoothed image stack to produce a 3-D mask corresponding to a single ciliated cell. In the case of images in which individual cells contained few cilia, and thus a low AAT signal, the mask was manually adjusted to outline the ciliated cell. To segment basal bodies within the ciliated cell, the contrast of the 16-bit centrin channel was enhanced to achieve 0.005% pixel saturation and converted to 8-bits. The image stack was convolved with a Laplacian of Gaussian kernel (smoothing radius 1 pixel), and the resulting 32-bit image was inverted and converted to 16-bits (Laplacian Stack). The Laplacian Stack was duplicated and converted to a MIP and the mean centrin signal within the ciliated cell mask was calculated. The contrast of the Laplacian Stack was adjusted to the mean centrin signal and the maximum intensity for a 16-bit image (65,535) and the image was then converted to 8-bits. Next, the 8-bit Laplacian Stack was convolved with a 3D maximum filter (isotropic in all dimensions; 1 pixel radius) and the resulting 3D maxima were used as seeds for seed region growing (SRG) of the Laplacian Stack (minimum object size=10 voxels; maximum object size=30 voxels; minimum object integrated density=3.5* (average object intensity)).

Authors' contributions

Together JS and MWK designed the *Xenopus* studies, which were carried out primarily by JS and YZ, with some contributions by MWK, DG wrote the confocal imaging quantification ImageJ subroutines and also provided advice on confocal imaging. MW, JS, and MWK were involved in overall final data analysis and manuscript preparation.

Acknowledgments

We thank Sergei Sokol for anti-centrin antibody, Feng-Qian Li for anti-Cby antibody, Kristen Kwan for the GFP-CAAX plasmid, Robin Dowell, Jim Huntley, and Sara Klymkowsky for collaborating with us on RNA SEQ sample analysis. The work was supported primarily by Collaborative Supplement to an NIH 3R01GM074746-06W1 Grant to Mark Winey and Mike Klymkowsky.

Appendix A. Supporting information

Supplementary data associated with this article can be found in the online version at http://dx.doi.org/10.1016/j.ydbio.2014.09.008.

References

Ariizumi, T., Takahashi, S., Chan, T.C., Ito, Y., Michiue, T., Asashima, M., 2009. Isolation and differentiation of Xenopus animal cap cells. Curr. Protoc. Stem Cell Biol. (Chapter 1: Unit 1D 5).
Avilion, A.A., Nicolis, S.K., Pevny, L.H., Perez, L., Vivian, N., Lovell-Badge, R., 2003. Multipotent cell lineages in early mouse development depend on SOX2 function. Genes Dev. 17 (1), 126–140.
Bradley, L., Sun, B., Collins-Racie, L., LaVallie, E., McCoy, J., Sive, H., 2000. Different activities of the frizzled-related proteins frzb2 and sizzled2 during Xenopus anteroposterior patterning. Dev. Biol. 227 (1), 118–132.
Carl, T.F., Dufton, C., Hanken, J., Klymkowsky, M.W., 1999. Inhibition of neural crest migration in Xenopus using antisense slug RNA. Dev. Biol. 213 (1), 101–115.
Cary, R.B., Klymkowsky, M.W., 1994. Differential organization of desmin and vimentin in muscle is due to differences in their head domains. J. Cell Biol. 126 (2), 445–456.
Cary, R.B., Klymkowsky, M.W., 1995. Disruption of intermediate filament organization leads to structural defects at the intersomite junction in Xenopus myotomal muscle. Development 121, 1041–1052.
Chang, J., Seo, S.G., Lee, K.H., Nagashima, K., Bang, J.K., Kim, B.Y., Erikson, R.L., Lee, K.-W., Lee, H.J., Park, J.-E., 2013. Essential role of Cenexin1, but not Odf2, in ciliogenesis. Cell Cycle 12 (4), 0–1.
Chu, D.T.W., Klymkowsky, M.W., 1989. The appearance of acetylated alpha-tubulin during early development and cellular differentiation in Xenopus. Dev. Biol. 136 (1), 104–117.
Chua, E.L., Young, L., Wu, W.M., Turtle, J.R., Dong, Q., 2000. Cloning of TC-1 (C8orf4), a novel gene found to be overexpressed in thyroid cancer. Genomics 69 (3), 342–347.
Chung, M.-I., Kwon, T., Tu, F., Brooks, E.R., Gupta, R., Meyer, M., Baker, J.C., Marcotte, E.M., Wallingford, J.B., 2014. Coordinated genomic control of ciliogenesis and cell movement by RFX2. eLife 3.
Chung, M.I., Peyrot, S.M., LeBoeuf, S., Park, T.J., McGary, K.L., Marcotte, E.M., Wallingford, J.B., 2012. RFX2 is broadly required for ciliogenesis during vertebrate development. Dev. Biol. 363 (1), 155–165.
Dent, J.A., Polson, A.G., Klymkowsky, M.W., 1989. A whole-mount immunocytochemical analysis of the expression of the intermediate filament protein vimentin in Xenopus. Development 105, 61–74.
Dixon, J.E., Allegrucci, C., Redwood, C., Kump, K., Bian, Y., Chatfield, J., Chen, Y.-H., Sottile, V., Voss, S.R., Alberio, R., 2010. Axolotl Nanog activity in mouse embryonic stem cells demonstrates that ground state pluripotency is conserved from urodele amphibians to mammals. Development 137 (18), 2973–2980.
Dubaissi, E., Papalopulu, N., 2011. Embryonic frog epidermis: a model for the study of cell–cell interactions in the development of mucociliary disease. Dis. Models Mech. 4 (2), 179–192.
Enjolras, C., Thomas, J., Chhin, B., Cortier, E., Duteyrat, J.L., Soulavie, F., Kernan, M.J., Laurencon, A., Durand, B., 2012. Drosophila chibby is required for basal body formation and ciliogenesis but not for Wg signaling. J. Cell Biol. 197 (2), 313–325.
Glinka, A., Wu, W., Delius, H., Monaghan, A.P., Blumenstock, C., Niehrs, C., 1998. Dickkopf-1 is a member of a new family of secreted proteins and functions in head induction. Nature 391 (6665), 357–362.
Ishikawa, H., Kubo, A., Tsukita, S., Tsukita, S., 2005. Odf2-deficient mother centrioles lack distal/subdistal appendages and the ability to generate primary cilia. Nat. Cell Biol. 7 (5), 517–524.
James-Zorn, C., Ponferrada, V.G., Jarabek, C.J., Burns, K.A., Segerdell, E.J., Lee, J., Snyder, K., Bhattacharyya, B., Karpinka, J.B., Fortriede, J., Bowes, J.B., Zorn, A.M., Vize, P.D., 2013. Xenbase: expansion and updates of the Xenopus model organism database. Nucl. Acids Res. 41 (D1), D865–D870.
Jones, E.A., Woodland, H.R., 1987. The development of animal cap cells in Xenopus: the effects of environment on the differentiation and the migration of grafted ectodermal cells. Development 101, 23–32.
Jung, Y., Bang, S., Choi, K., Kim, E., Kim, Y., Kim, J., Park, J., Koo, H., Moon, R.T., Song, K., 2006. TC1 (C8orf4) enhances the Wnt/β-catenin pathway by relieving antagonistic activity of Chibby. Cancer Res. 66 (2), 723–728.
Kanai-Azuma, M., Kanai, Y., Gad, J.M., Tajima, Y., Taya, C., Kurohmaru, M., Sanai, Y., Yonekawa, H., Yazaki, K., Tam, P.P., Hayashi, Y., 2002. Depletion of definitive gut endoderm in Sox17-null mutant mice. Development 129 (10), 2367–2379.
Karnovsky, A., Klymkowsky, M.W., 1995. Anterior axis duplication in Xenopus induced by the over-expression of the cadherin-binding protein plakoglobin. Proc. Natl. Acad. Sci. USA 92 (10), 4522–4526.
Kim, K.D., Lake, B.B., Haremaki, T., Weinstein, D.C., Sokol, S.Y., 2012. Rab11 regulates planar polarity and migratory behavior of multiciliated cells in Xenopus embryonic epidermis. Dev. Dyn. 241 (9), 1385–1395.
Klymkowsky, M.W., 2005. Beta-catenin and its regulatory network. Hum. Pathol. 36, 225–227.
Korinek, V., Barker, N., Morin, P.J., van Wichen, D., de Weger, R., Kinzler, K.W., Vogelstein, B., Clevers, H., 1997. Constitutive transcriptional activation by a beta-catenin-Tcf complex in APC-/- colon carcinoma. Science 275 (5307), 1784–1787.
Kormish, J.D., Sinner, D., Zorn, A.M., 2010. Interactions between SOX factors and Wnt/β-catenin signaling in development and disease. Dev. Dyn. 239 (1), 56–68.
Kunimoto, K., Yamazaki, Y., Nishida, T., Shinohara, K., Ishikawa, H., Hasegawa, T., Okanoue, T., Hamada, H., Noda, T., Tamura, A., 2012. Coordinated ciliary beating requires *Odf2* mediated polarization of basal bodies via basal feet. Cell 148 (1), 189–200.
Li, F.Q., Mofunanya, A., Fischer, V., Hall, J., Takemaru, K., 2010. Nuclear-cytoplasmic shuttling of Chibby controls beta-catenin signaling. Mol. Biol. Cell 21 (2), 311–322.

Ligon, L.A., Karki, S., Tokito, M., Holzbaur, E.L.F., 2001. Dynein binds to β-catenin and may tether microtubules at adherens junctions. Nat. Cell Biol. 3 (10), 913–917.
Lombardi, R., da Graca Cabreira-Hansen, M., Bell, A., Fromm, R.R., Willerson, J.T., Marian, A.J., 2011. Nuclear plakoglobin is essential for differentiation of cardiac progenitor cells to adipocytes in arrhythmogenic right ventricular cardiomyopathy. Circ. Res. 109 (12), 1342–1353.
Love, D., Li, F.Q., Burke, M.C., Cyge, B., Ohmitsu, M., Cabello, J., Larson, J.E., Brody, S.L., Cohen, J.C., Takemaru, K., 2010. Altered lung morphogenesis, epithelial cell differentiation and mechanics in mice deficient in the Wnt/beta-catenin antagonist Chibby. PLoS One 5 (10), e13600.
Mancini, M., Leo, E., Takemaru, K.-I., Campi, V., Borsi, E., Castagnetti, F., Gugliotta, G., Santucci, M.A., Martinelli, G., 2013. Chibby drives β catenin cytoplasmic accumulation leading to activation of the unfolded protein response in BCR-ABL1+ cells. Cell. Signal.
Mayor, R., Guerrero, N., Young, R.M., Gomez-Skarmeta, J.L., Cuellar, C., 2000. A novel function for the Xslug gene: control of dorsal mesendoderm development by repressing BMP-4. Mech. Dev. 97 (1–2), 47–56.
Mbom, B.C., Nelson, W.J., Barth, A., 2013. β-. 3hnl functhe centrosome. BioEssays 35 (9), 804–809.
Merriam, J.M., Rubenstein, A.B., Klymkowsky, M.W., 1997. Cytoplasmically anchored plakoglobin induces a WNT-like phenotype in Xenopus. Dev. Biol. 185 (1), 67–81.
Mofunanya, A., Li, F.Q., Hsieh, J.C., Takemaru, K., 2009. Chibby forms a homodimer through a heptad repeat of leucine residues in its C-terminal coiled-coil motif. BMC Mol. Biol. 10, 41.
Mokhtarzada, S., Yu, C., Brickenden, A., Choy, W.-Y., 2011. Structural characterization of partially disordered human Chibby: insights into its function in the Wnt-signaling pathway. Biochemistry 50 (5), 715–726.
Murray, S.A., Gridley, T., 2006. Snail1 gene function during early embryo patterning in mice. Cell Cycle 5 (22), 2566–2570.
Nieuwkoop, P.D., Faber, J., 1967. Normal Table of Xenopus laevis (Daudin): A Systematical and Chronological Survey of the Development from the Fertilized Egg till the End of Metamorphosis. Amsterdam Publishing Company, Amsterdam, New York (republished in 1994 by Garland Publishing).
Okita, K., Ichisaka, T., Yamanaka, S., 2007. Generation of germline-competent induced pluripotent stem cells. Nature 448 (7151), 313–317.
Paoletti, A., Moudjou, M., Paintrand, M., Salisbury, J.L., Bornens, M., 1996. Most of centrin in animal cells is not centrosome-associated and centrosomal centrin is confined to the distal lumen of centrioles. J. Cell Sci. 109 (Pt 13), 3089–3102.
Satir, P., Christensen, S.T., 2007. Overview of structure and function of mammalian cilia. Annu. Rev. Physiol. 69, 377–400.
Scerbo, P., Girardot, F., Vivien, C., Markov, G.V., Luxardi, G., Demeneix, B., Kodjabachian, L., Coen, L., 2012. Ventx factors function as nanog-like guardians of developmental potential in Xenopus. PloS one 7 (5), e36855.
Shi, J., Severson, C., Yang, J., Wedlich, D., Klymkowsky, M.W., 2011. Snail2 controls BMP- and Wnt-dependent mesodermal induction of neural crest. Development 138, 3135–3145.
Singh, A.M., Li, F.-Q., Hamazaki, T., Kasahara, H., Takemaru, K.-I., Terada, N., 2007. Chibby, an antagonist of the Wnt/Œ ≤ -catenin pathway, facilitates cardiomyocyte differentiation of murine embryonic stem cells. Circulation 115 (5), 617–626.
Sinner, D., Rankin, S., Lee, M., Zorn, A.M., 2004. Sox17 and beta-catenin cooperate to regulate the transcription of endodermal genes. Development 131, 3069–3080.
Sive, H., 2011. 'Model' or 'tool'? New definitions for translational research. Dis. Models Mech. 4 (2), 137–138.
Sive, H.L., Grainger, R.M., Harland, R.M., 2000. Early Development of *Xenopus laevis*: A Laboratory Manual. Cold Spring Harbor Laboratory Press, Cold Spring Harbor.
Steere, N., Chae, V., Burke, M., Li, F.-Q., Takemaru, K.-I., Kuriyama, R., 2012. A Wnt/beta-catenin pathway antagonist Chibby binds Cenexin at the distal end of mother centrioles and functions in primary cilia formation. PLoS ONE 7 (7), e41077.
Steinman, R.M., 1968. An electron microscopic study of ciliogenesis in developing epidermis and trachea in the embryo of Xenopus laevis. Am. J. Anat. 122 (1), 19–55.
Stubbs, J.L., Davidson, L., Keller, R., Kintner, C., 2006. Radial intercalation of ciliated cells during Xenopus skin development. Development 133 (13), 2507–2515.
Sullivan, S.A., Akers, L., Moody, S.A., 2001. foxD5a, a Xenopus Winged Helix Gene, maintains an immature neural ectoderm via transcriptional repression that is dependent on the C-terminal domain. Dev. Biol. 232 (2), 439–457.
Sunde, M., McGrath, K.C.Y., Young, L., Matthews, J.M., Chua, E.L., Mackay, J.P., Death, A.K., 2004. TC-1 is a novel tumorigenic and natively disordered protein associated with thyroid cancer. Cancer Res. 64 (8), 2766–2773.
Takahashi, K., Tanabe, K., Ohnuki, M., Narita, M., Ichisaka, T., Tomoda, K., Yamanaka, S., 2007. Induction of pluripotent stem cells from adult human fibroblasts by defined factors. Cell 131 (5), 861–872.
Takemaru, K., Yamaguchi, S., Lee, Y.S., Zhang, Y., Carthew, R.W., Moon, R.T., 2003. Chibby, a nuclear beta-catenin-associated antagonist of the Wnt/Wingless pathway. Nature 422 (6934), 905–909.
Takemaru, K.-I., Fischer, V., Li, F.-Q., 2009. Fine-tuning of nuclear beta-catenin by Chibby and 14-3-3. Cell Cycle 8 (2), 210–213.
Vandepoele, K., Staes, K., Andries, V., Van Roy, F., 2010. Chibby interacts with NBPF1 and clusterin, two candidate tumor suppressors linked to neuroblastoma. Exp. Cell Res. 316 (7), 1225–1233.
Vize, P.D., Jones, E.A., Pfister, R., 1995. Development of the Xenopus pronephric system. Dev. Biol. 171 (2), 531–540.
Voronina, V.A., Takemaru, K., Treuting, P., Love, D., Grubb, B.R., Hajjar, A.M., Adams, A., Li, F.Q., Moon, R.T., 2009. Inactivation of Chibby affects function of motile airway cilia. J. Cell Biol. 185 (2), 225–233.
Yanai, I., Peshkin, L., Jorgensen, P., Kirschner, M.W., 2011. Mapping gene expression in two Xenopus species: evolutionary constraints and developmental flexibility. Dev. Cell 20 (4), 483–496.
Ye, X., Wu, F., Wu, C., Wang, P., Jung, K., Gopal, K., Ma, Y., Li, L., Lai, R., 2014. β-Catenin, a Sox2 binding partner, regulates the DNA binding and transcriptional activity of Sox2 in breast cancer cells. Cell. Signal. 26 (3), 492–501.
Yoshimura, S.-i., Egerer, J., Fuchs, E., Haas, A.K., Barr, F.A., 2007. Functional dissection of Rab GTPases involved in primary cilium formation. J. Cell Biol. 178 (3), 363–369.
Zhang, C., Basta, T., Jensen, E.D., Klymkowsky, M.W., 2003. The beta-catenin/VegT-regulated early zygotic gene Xnr5 is a direct target of SOX3 regulation. Development 130 (23), 5609–5624.
Zhang, C., Basta, T., Klymkowsky, M.W., 2005. SOX7 and SOX18 are essential for cardiogenesis in Xenopus. Dev. Dyn. 234, 878–891.
Zhang, C., Carl, T.F., Trudeau, E.D., Simmet, T., Klymkowsky, M.W., 2006. An NF-kappaB and slug regulatory loop active in early vertebrate mesoderm. PLoS ONE 1, e106.
Zhang, C., Klymkowsky, M.W., 2007. The Sox axis, nodal signaling, and germ layer specification. Differentiation 75, 536–545.
Zhang, C., Klymkowsky, M.W., 2009. Unexpected functional redundancy between Twist and Slug (Snail2) and their feedback regulation of NF-kappaB via Nodal and Cerberus. Dev. Biol. 331 (2), 340–349.
Zorn, A.M., Barish, G.D., Williams, B.O., Lavender, P., Klymkowsky, M.W., Varmus, H.E., 1999. Regulation of Wnt signaling by Sox proteins: XSox17 alpha/beta and XSox3 physically interact with beta-catenin. Mol. Cell 4 (4), 487–498.